

GLOBAL JOURNAL OF ENGINEERING SCIENCE AND RESEARCHES

REINFORCEMENT OF BLACK COTTON SUBGRADE SOIL USING COIR GEOTEXTILE AND ANALYSIS OF RUT DEPTH BY LWT

Madhu Singh^{*1} & Ravi Kumar Gautam²
*1&2 Assistant Professor, AIMT, Lucknow

ABSTRACT

Soil in the dynamic nature always present different behavior from static conditions. Liquefaction can be controlled by reinforcing saturated sands is one of the solutions to mitigate liquefaction potential. Scrap recycle materials are some kinds of reinforcing materials such as tire chips. In addition to mitigation effects, the reinforcing materials also cause an improvement in dynamic properties of the soils hence reducing the chances of liquefaction. A series of one dimensional 1-g shaking table model tests were conducted on sand and sand mixed tire chips. Four different percentages of sand-tire chips were tested and Shear modulus and damping ratio degradation curves were presented in the hysteresis loops too. Analysis concluded damping ratio increases with increasing tire chips content in mixture. Also at the certain shear strain amplitude, shear modulus of reinforced soil decreases with increasing percentage of tire chips.

Keywords : *Tire chips, liquefaction, shaking table.*

I. INTRODUCTION

When saturated clean sand deposit is subjected to seismic loading, the pore water pressure gradually increases until liquefaction happens and settlement occurs during and after an earthquake. The mentioned problem is attributed to rearrangement of grains and redistribution of voids within the soils. Over the years many methods have been presented to increase liquefaction resistance. However the main methods utilized in liquefaction mitigation are classified as densification, solidification, drainage and reinforcement techniques. Utilizing tire chips in soils is a kind of soil reinforcement which has a wide range of application. Many research works have been performed to achieve fundamental engineering properties of soil- rubber mixture, such as compaction characteristics, permeability, compressibility, modulus of elasticity, and Poisson's ratio conducted a series of resonant column test to obtain shear modulus and damping ratio of sand reinforced with rubber. They expressed that shear modulus and damping ratio of the mixtures is strongly influenced by the percentage of the rubber inclusion. Few studies have been performed on the effect of adding tire chips in mitigating the liquefaction potential of sand. Hyodo et al. (2007) carried out undrained cyclic triaxial tests on sand sample reinforced with tire chips. They found out that tire chips control build-up of excess pore water pressure of the mixture during shear. They obtained that for sand fraction (i.e. sand volume /tire chips volume) lower than 50 percent, liquefaction does not occur at all. Studies on liquefaction resistance of reinforced soils with tire chips have been so far limited to almost element tests. In this paper a series of 1g shaking table tests were carried out to investigate on the effect of tire chips -sand mixture in reducing liquefaction potential, settlements after earthquake and pore water generation.

II. SHAKING TABLE AND MATERIALS

2.1. Model configuration and instrumentation

Figure 1 illustrates shaking table and its instruments. Container is made of Plexiglas with inner dimensions of 200×50×70 cm. A plastic plate was rigidly fixed at the center of container to separate reinforced and unreinforced parts from each other and waterproofing carefully. So two models (reinforced and unreinforced) can be tested at once with the same input acceleration.

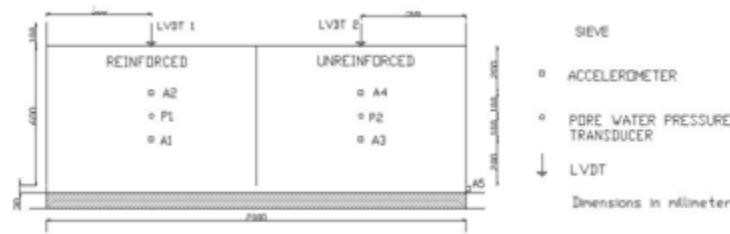


Figure 1.General view of shaking table model

2.2. Materials

The tire chips used in this study was made from discarded tires. The particles shape was very irregular and angular. The tire chips particles have negligible water absorption, and very small volumetric compression due to isotropic pressure. Table 1 demonstrates physical properties of tire chips.

Table 1. Physical properties of tire chips material

Material	D ₁₀ (mm)	D ₃₀ (mm)	C _c	C _u	G _s
Tire chips	2.1	3.9	0.99	2.05	1.16

Firoozkuh No.161 sand was used for the mixture in reinforced side, and pure sand in unreinforced side. Table 2 demonstrates physical properties of sand.

Table 2.physical properties of sand material

Material	G _s	e _{max}	e _{min}	C _c	C _u	D ₅₀ (mm)
Sand	1.16	0.874	0.548	0.97	2.58	0.3

2.3. Experimental procedure

Uchimura et al. (2007) presented following relation to calculate mixture ratio of tire chips that were evaluated by the dry weight of the tire chips relative to the total mixture material:

$$TC_r = \frac{M_{TC}}{M_s + M_{TC}} \tag{1}$$

(TC_r : Tire chips content, M_{TC} : Weight of tire chips ,

M_s : Weight of Firoozkuh sand).

In this study 4 mixture ratio (TCr=10%, TCr=20%, TCr=30% and TCr=40%) were selected. Maximum mixture ratio was limited to 40 percent, because if tire chips content were higher, the sand could not fill the entire voids among tire chips particles and the model became non-uniform.

Relative density of tire chips-sand mixture was calculated by following relation:

(e_s : sand void ratio, e_{max} : maximum void ratio of sand

$$D_r = \frac{(e_{\max} - e_s)}{(e_{\max} - e_{\min})} \quad (2)$$

(e_s : sand void ratio, e_{\max} : maximum void ratio of sand

, e_{\min} : minimum void ratio of sand). Where e_s can be calculated as:

$$e_s = \frac{V_{Total} - V_s - V_{Tc}}{V_s} \quad (3)$$

(V_{Total} : Total volume of mixture, V_s : Volume of sand particles , V_{Tc} :Volume of Tire chips particles)

Both of unreinforced (pure sand) and reinforced (tire chips-sand mixture) models were prepared by wet tamping method, in which soil is mixed with 5% water.

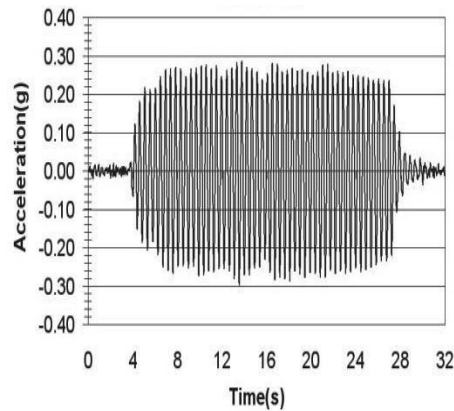
Each model (reinforced or unreinforced) was prepared in six layers. The required weight for each layer was considered based on the desired density (equivalent value of the maximum void ratio or zero relative density) and exact volume of the layer. Each portion was placed into the model container and then tamped with light trowel to reach desired level.

Carbon dioxide (CO₂) was allowed to pass through the specimen at a low pressure in order to replace the air that trapped in the pores of the specimen. Then water was allowed to flow upward through the bottom of the container at low pressures in order to flush out the CO₂ that cause increasing the final degree of saturation. Vibration with approximate uniform amplitude and 2.1 Hz freq was manually applied to the container (the shaking table was designed to vibrate at around 2 Hz frequencies).

III. TEST RESULTS AND DISCUSSION

3.1 Time history of acceleration

Figure 2 is a typical plot of time history of base acceleration measured by accelerometers (a5). It is noticeable that in all models base acceleration was continued for 23 second. Results indicated that acceleration within the soil tends to be increased towards the soil surface. On the other hand, after initial liquefaction (that occurred at un-reinforced models and also reinforced model with TCr=10%), acceleration is decreased due to the increase in excess pore water Pressure.



(d)

Figure 2. Typical Time History of Base Acceleration

3.2. Shear stress-strain relationship

From the original shear beam equation, shear stress τ at any depth z may be written as the integration of density (ρ) times acceleration (\ddot{u}) through higher levels (Eq.4).

$$\tau = \int \rho u \ddot{u} dz \quad (4)$$

0

A linear fit is recommended between adjacent pairs of instruments, which may be extrapolated from the top pair to surface (Eq. (5)).

$$u(z) = u_1 + \frac{(u_2 - u_1)}{(z_2 - z_1)} (z - z_1) \quad (5)$$

Shear stress is evaluated using Zeghal and Elgamal's expression with the interpolated surface acceleration obtained from Eq. (5) with $z=0$:

$$\tau(z) = \rho \int_0^z \left(\frac{u_2 - u_1}{z_2 - z_1} + u_1 \right) dz \quad (6)$$

If only two instruments are present in a given soil layer, a simple first order approximation must be applied to calculate shear strain:

$$\gamma = \frac{(u_2 - u_1)}{(z_2 - z_1)} \quad (7)$$

This applies for any point between instruments 1 and 2, and as such is more appropriate for the midpoint. Figure 3 shows Stress–strain loops at P1 and P2 in reinforced and unreinforced sides of test with $TC_r=40\%$.

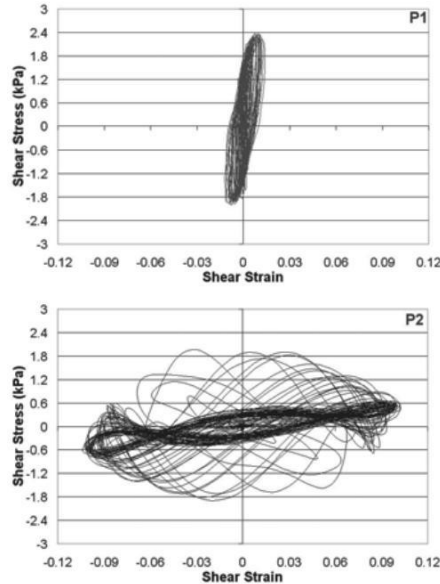


Figure 3. Shear stress-strain loops for unreinforced and reinforced models with $TC_r=40\%$

It is clear that the hysteresis loops in unreinforced model tends to become progressively flatter and narrower as the sample begins to liquefy and display a clear reduction in stiffness. One reason for the good performance of sand-tire chips mixture in reducing generation of excess pore water pressure and increasing liquefaction resistance is high permeability of reinforced mixture, as compared with the pure sand. Another reason is probably that the stiffness of tire chip particles is less than that of sand grains, consequently allowing some volume compression under developed excess pore water pressure. Thus the volume compression of tire chip produces a situation similar to drainage or dewatering which decreases the extent of excess pore water pressure (Towhata, 2008).

3.3. Shear modulus and damping ratio

Shear modulus is obtained from the ratio of the difference in maximum and minimum stress and strain developed in desired loop.

$$G = \frac{\tau_{max} - \tau_{min}}{\gamma_{max} - \gamma_{min}} \quad (8)$$

To calculate the damping ratio in each cycle of motion (Eq. 9), first, dissipated energy (ΔW) & absorbed energy ($W_{elastic}$) must be calculated (Fig. 4).

$$D = \frac{1}{4\pi} \frac{\Delta W}{W_{elastic}} = \frac{1}{4\pi} \frac{\oint \tau d\gamma}{0.125 \times \Delta\tau \times \Delta\gamma}$$

$$D = \frac{1}{4\pi} \frac{\Delta W}{W_{elastic}} = \frac{1}{4\pi} \frac{\oint \tau d\gamma}{0.125 \times \Delta\tau \times \Delta\gamma} \quad (9)$$

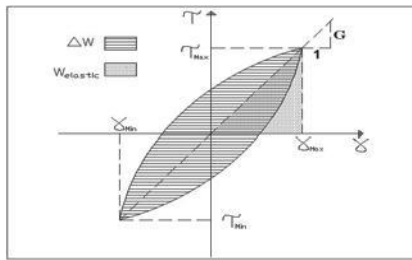
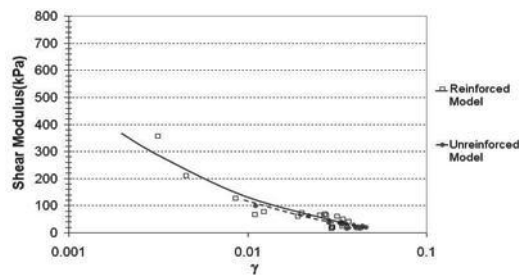
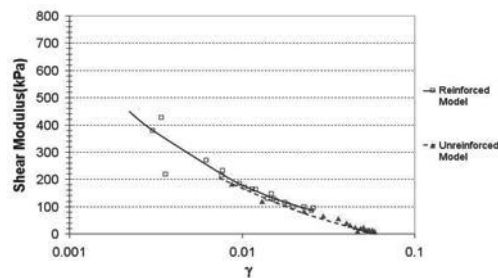


Figure 4. Definition of Damping ratio and Shear Modulus

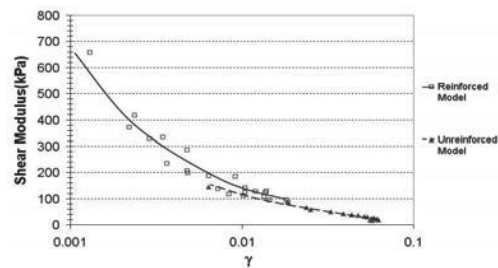
Shear modulus and damping ratios at 0.3m depth for all reinforced and unreinforced models are shown in Fig. 5.



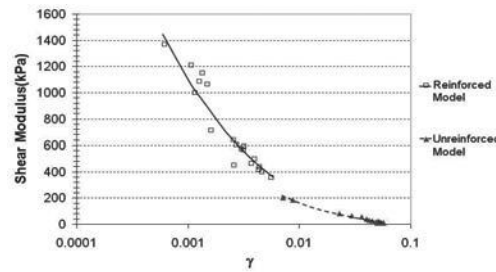
(a)



(b)



(c)



(d)

Figure 5. Shear modulus of Reinforced and Unreinforced models: a) TCr=10% b) TCr=20% c) TCr=30% d) TCr=40%

As it is depicted in Fig. 11, the shear modulus curve of reinforced model is placed over the unreinforced one. Also, increasing content ratio of tire chips in mixture causes shear modulus degradation curves of reinforced models shift to left side of strain axis and consequently obtained shear strain is reduced.

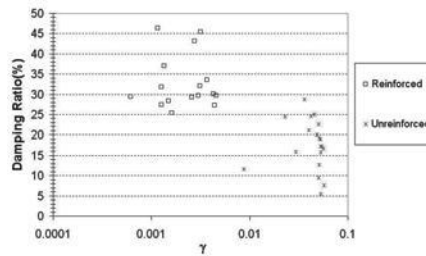


Figure 6. Damping ratio of Reinforced and Unreinforced model with TCr=40%.

Damping ratio curve of reinforced and un-reinforced model with TCr=40% are presented in Fig. 6. At all models, the scattering of damping ratio values is high. As a general result, value of damping ratio is reduced by increasing strain amplitude. This process is similar to conclusions of Brennan (2004), which explained mentioned phenomena happens when the soil particles lose contact each other due to increase of pore water pressure and consequently cause frictional energy of soil skeleton reduced and since damping ratio is the ratio of dissipated energy to absorbed energy therefore damping ratio is reduced.

3.3.1. Mean damping ratio

Due to observing relatively irregular and non-uniform trends of damping ratios versus shear strain that has occurred because of various reasons such as high shear strain amplitude and sudden increase in pore water pressure, a new parameter is defined as the mean value of damping ratio by Sabermahani et al. (2009) to compare the values of damping ratio of reinforced models with each other. The values of mean damping ratio versus tire chips content ratio of reinforced model tests are plotted in Fig. 7. Results show that value of the mean damping ratio at the shear strain range of 10^{-2} , is increased with increase in tire chips content.

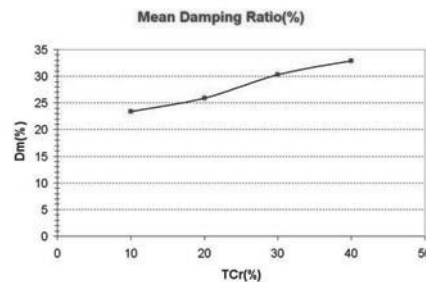


Fig.7. Mean damping ratio of Reinforced Models

IV. CONCLUSIONS

1. It seems tire chips can control the build-up of excess pore water pressure of the mixture during earthquake and increase liquefaction resistance.
2. Although unreinforced sand shows reducing in stiffness during earthquake due to rapid build-up of excess pore water pressure, no sign of losing in stiffness was observed in reinforced sand with tire chips.
3. Maximum shear modulus of reinforced soil increased with increasing tire chips content in mixture due to decreasing excess pore water generation.
4. Mean damping ratio is increased with increasing tire chips content in sand-tire chips mixture.

REFERENCES

1. Ghiassian, H. and Ghazi, F. 2009. Liquefaction analysis of fine sand reinforced with carpet waste fibers under triaxial tests, 2nd International Conference on New Developments in Soil Mechanics and Geotechnical Engineering, Near East University, Nicosia, North Cyprus, pp. 448-455.
2. Zheng-Yi, F. and Sutter, G. Dynamic Properties of Granulated Rubber/Sand Mixtures, Geotechnical Testing Journal, GTJODJ, Vol. 23, No. 3, September 2000, pp.338-344.
3. Hyodo, M., Yamada, S., Okamoto, M. 2007, Undrained cyclic shear properties of Tire chips–sand mixture, Int. workshop on scrap Tire derived geomaterials, Yokosuka, Japan.
4. Bahadori, H. and Motamedi, H. 2011, An investigation on the effects of geogrid and geogrid- geomembrane geocomposite on the reduction of settlement due to liquefaction”, 6 th International Conference on Seismology and Earthquake Engineering, Tehran, Iran
5. Uchimura, M. ,Chi, N.A. ,Nirmalan ,S. ,Sato ,T. ,Mediani , M., Towhata , I. 2007. Shaking table test on the effect of tire chips and sand mixture in increasing liquefaction resistance and mitigation uplift of pipe, International workshop on scrap tire derived geomaterials, Yokosuka, Japan.
6. Zeghal, M. and Elgamal, A.W. 1994. Analysis of site liquefaction using earthquake records. J. Geotech. Eng., 120(6), 996–1017.
7. Towhata, I. 2008. Geotechnical earthquake engineering, Springer First Edition.
8. Brennan, A. J. 2004. Vertical drains as a countermeasure to earthquake-induced soil liquefaction. PhD thesis, Univ. of Cambridge, Cambridge, U.K.
9. Sabermahani, M., Ghalandarzadeh, A., Fagher, A. 2009. Experimental study on seismic deformation modes of reinforced-soil walls. j. Geotextiles and Geomembranes., 27(9), 121-136.